Radio-frequency properties of stacked long Josephson junctions with nonuniform bias current distribution

Filatrella, G; Pedersen, Niels Falsig

Published in:
Journal of Applied Physics

Link to article, DOI:
10.1063/1.370210

Publication date:
1999

Document Version
Publisher's PDF, also known as Version of record

Radio-frequency properties of stacked long Josephson junctions with nonuniform bias current distribution

G. Filatrella[a] and N. F. Pedersen[b]
Department of Physics, Technical University of Denmark, DK-2800 Lyngby, Denmark

(Received 15 September 1998; accepted for publication 5 January 1999)

We have numerically investigated the behavior of stacks of long Josephson junctions considering a nonuniform bias profile. In the presence of a microwave field the nonuniform bias, which favors the formation of fluxons, can give rise to a change of the sequence of radio-frequency induced steps. The amplitude of the steps is enhanced when the external frequency matches the fluxon shuttling regime. © *1999 American Institute of Physics.* [S0021-8979(99)05507-3]

I. INTRODUCTION

Stacked Josephson junctions have attracted a lot of interest recently both because of interesting nonlinear properties and because of the potential applications.[1–7] Among the applications probably the most interesting is the possibility to achieve stable phase locking of several junctions in the fluxon regime so to achieve a microwave generator. The stack may be the key ingredient to phase lock the junctions and thus providing both high power and high impedance to match the external load.

The stacked junctions, however, may give rise to some peculiar current distributions–depending on the geometry and the bias conditions[8]–that affect the microwave properties in a more complicated way than for single junctions. This article intends to address such problems.

In Ref. 8 it was concluded that for the particular sample geometry used (i.e., two overlap junctions with the possibility to independently bias both junctions) the bias current distribution could be either the normal one for single long junctions without a ground plane, i.e., with spikes at the edges, it could be a uniform distribution, or it could be a distribution intermediate between the two. The distribution depends on how the bias current is fed into the junctions in the stack. In Ref. 8 the consequences of such complicated distributions for the magnetic field diffraction pattern was investigated. Here we will investigate how it affects the microwave coupling.

II. THE MODEL

The model that we will employ is the magnetic coupling model,[9] that in normalized units reads:

$$\phi^1_{tt} - \phi^1_{xx} + \sin\phi^1 = -\alpha\phi^1_t + \gamma + \epsilon\phi^2_{xx}, \tag{1}$$

$$\phi^2_{tt} - \phi^2_{xx} + \sin\phi^2 = -\alpha\phi^2_t + \gamma + \epsilon\phi^1_{xx}, \tag{2}$$

where ϕ is the phase difference across the junctions, the coordinate x and time t are measured in units of the Josephson penetration length and inverse plasma frequency of the junction, respectively, α is the dissipation constant, ϵ the coupling constant of the two junctions,[9] γ the normalized bias current. The radio-frequency (rf) term enters through the magnetic field,[10] which has proved the most effective way to couple fluxon motion to the external drive.[11] The magnetic field modifies the boundary conditions as follows:

$$\phi^1_x(0) = -\phi^1_x(l) = 2\pi\eta_{\rm rf}\sin(\omega t)(1+\epsilon), \tag{3}$$

$$\phi^2_x(0) = -\phi^2_x(l) = 2\pi\eta_{\rm rf}\sin(\omega t)(1+\epsilon), \tag{4}$$

where $\eta_{\rm rf}$ is the normalized amplitude of the magnetic component of the incident microwave, and ω is the frequency of the drive.

Figure 1 shows the two extremes of the current distribution for a junction of normalized length 10. One is the spiky distribution[7,12] (ℓ is the length of the junction, $0 \leqslant x \leqslant l$ the spatial coordinate):

$$I \propto \left(\sqrt{x(l-x)}\right)^{-1} \tag{5}$$

and the other is the uniform one.

Figure 2 shows a calculation of the current–voltage (I–V) curve for the two bias current distributions. We note that the nonuniform bias current with spikes induces zero field steps. This is because large bias current at the edges acts as a magnetic field boundary condition ($\Phi_x \propto H$) and creates fluxons. (The zero fluxon mode becomes unstable towards the formation of a fluxon–antifluxon pair.) The I–V curve is obtained by decreasing the current from high values. The part of the I–V curve marked by symbols (stars) is obtained by increasing the current from the kinks in the I–V curve. For the uniform current distribution a completely smooth I–V curve is obtained with the same calculation procedure (dashed line). The zero field steps can only be obtained through imposing corresponding initial conditions or by waiting sufficiently long time for an instability to occur. The difficulty of obtaining the ZFS in some cases is well known also from experiments.[13]

III. THE EFFECT OF THE MICROWAVE FIELD

Figure 3 shows an example of the effect of applying a rf signal to the system of Fig. 2, i.e., a stack of two junctions. The parameters are as follows: $l=10$, $\alpha=0.1$, $\eta_{\rm rf}=0.3$,

[a]Permanent address: Unità INFM Salerno-Facoltà di Scienze, Università del Sannio, Benevento, Italy; electronic mail: giofil@physics.unisa.it
[b]Electronic mail: nfp@fysik.dtu.dk

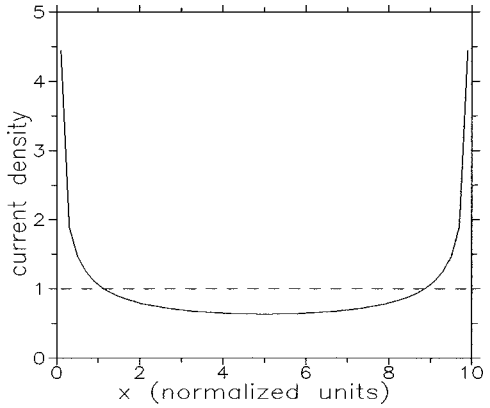

FIG. 1. The bias most extreme profiles: the uniform profile (dashed line) and the spiky profile of Eq. (5) (solid line).

$\omega=1$. The frequency is chosen so that it is somewhat higher than the fundamental fluxon frequency, $\omega_{fl}=2\pi/l=0.63$. Because of the ''magnetic'' boundary conditions the first rf induced step to be expected is at $V=2$.[10] Figure 4 shows schematically why this is the case. The upper part shows the (fixed) rf signal. The lower part shows the fluxon trajectory. For the lowest voltage phase locking, a fluxon must go back and forth during three rf periods. Since the total phase shift is 4π the corresponding voltage corresponds to $V\propto 4\pi u$. Figure 3 shows that indeed a large step occurs at $V=2$ both for the nonuniform and for the uniform current distribution. This large step is a consequence of the phase locking involving three fluxons in the manner shown in Fig. 4. Because the phase locking involves $V=2$ it is necessary to use the third ZFS for the chosen example. We note that the I–V curves are quite different for the two current distributions. One reason for the difference is that fluxon creation and motion is important for the phase locking, and the two bias current distributions behave quite differently in that respect. In particular we note that one rf-induced step (at $V=4$) is found only for the nonuniform current distribution. It seems difficult to find generally applicable rules for the height of the rf induced steps for the two current distributions, but typically

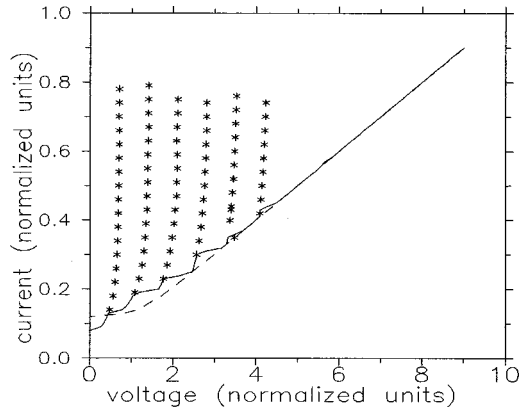

FIG. 2. The $I-V$ curves with uniform bias (dashed line) and the nonuniform (solid line) for a two-junction stack obtained by decreasing the bias current. We also show the full height of the ZFS, obtained increasing the bias with nonuniform profile, with marks. In this figure, $L=10$, $\alpha=0.1$, and $\epsilon=0.3$.

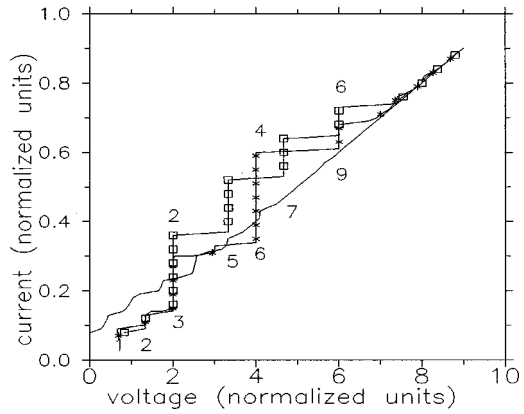

FIG. 3. The effect of a microwave applied through the boundary conditions for the uniform (squares) and nonuniform (stars) bias. We also show the unperturbed (i.e., without applied microwave) curve for reference (solid line). The numbers above the curve refer to the rf induced steps order, and the numbers below the curve to the number of fluxons. Parameters of the simulations are: $L=10$, $\alpha=0.1$, $\epsilon=0.3$, and $\eta_{\rm rf}=0.3$.

the stability of rf-induced steps (the locking range) is smaller with the nonuniform current distribution. Typically, a switching occurs to a rf-induced step connected with a higher order zero field step. This is qualitatively understandable since the spikes in the current distribution make it easier to introduce an extra fluxon at the boundaries. We note that large rf-induced steps are also found near $V=4$ and 6 These are obviously harmonic extensions of the processes near $V=2$ and will be discussed below. Figure 5 shows the effect of varying the frequency. Figure 5(a) shows the third ZFS while Fig. 5(b) shows the height of the fundamental $n=2$ rf induced step corresponding to the nonuniform current distribution. We note that quite obviously the height of the rf-induced step is connected with the resonance corresponding to the third ZFS. The dynamic process with the three resonating fluxons is shown in Fig. 4. Also the $n=4$ and $n=6$ rf induced steps are enhanced because of the interaction with fluxons. Also for these steps the maximum height of the rf-induced steps correspond approximately to the center of voltage range of $n=6$ and 9 ZFS, respectively. The dynamical picture corresponds to Fig. 4 but with six and nine fluxons instead of three. We have confirmed the dynamic picture

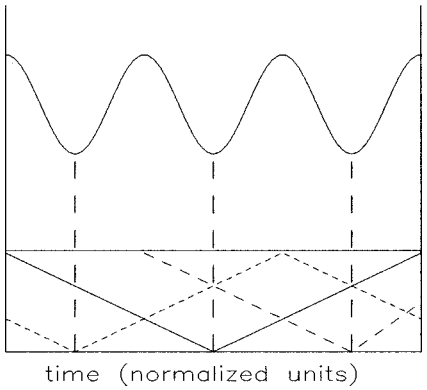

FIG. 4. A sketch of the dynamical configurations in the phase-locked modes. In the upper part of the figure the external drive is shown and in the lower part the schematic fluxon trajectories.

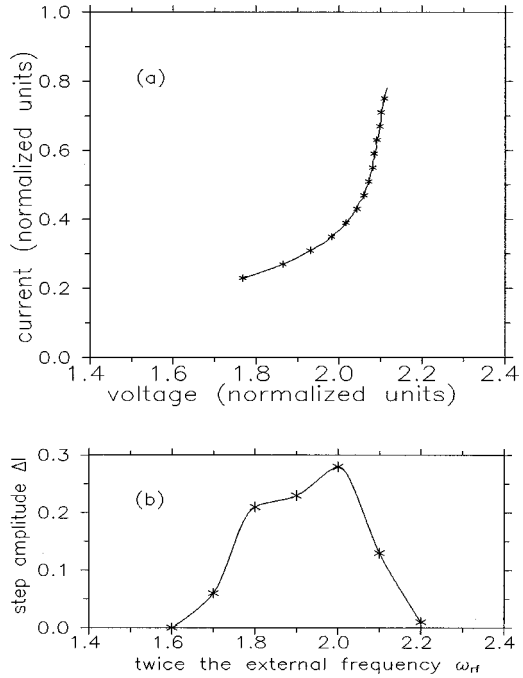

FIG. 5. The profile of the third ZFS (a) and the amplitude of the Shapiro induced steps as a function of the applied frequency (b). The scale in the first part of the figure has been doubled to compare with the voltage scale of the ZFS. The solid line serves as a guide for the eye. Parameters of the simulations are: $L=10$, $\alpha=0.1$, $\epsilon=0.3$, and $\eta_{rf}=0.3$.

described above with other lengths and rf frequencies. Thus for $L=7$ the maximum height of the rf-induced step was found at $\omega=1.4$ in full agreement with the discussion above. Figure 6 shows for low rf power the qualitative behavior of the rf induced steps for the two current distributions. The parameters are: $L=10$, $\alpha=0.1$, $\epsilon=0.3$, and $\eta_{rf}=0.2$. Note the switching of the ZFS No. 1 to the ZFS No. 2 due to the creation of an extra fluxon.

IV. CONCLUSION

In conclusion we have demonstrated that the profile of the bias current is essential in simulating the effect of an external rf drive even if the drive itself is introduced through

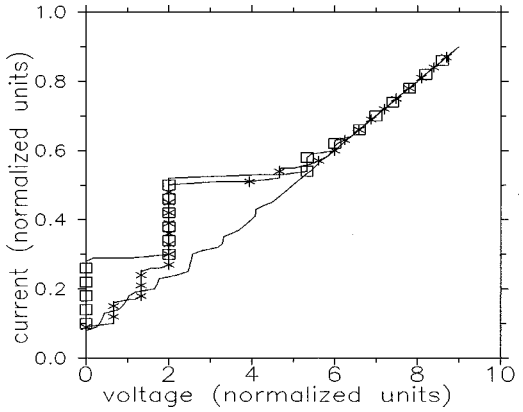

FIG. 6. The I–V curve of a stack of two junctions with the same parameters as Fig. 3 but with smaller rf power ($\eta_{rf}=0.2$).

the boundary conditions. In other words we simulated the effect of an rf magnetic field with two profiles of the direct-current (dc) bias and we have found that: (a) the fluxons are spontaneously formed for the nonuniform bias; (b) the so formed fluxons easily interact with the oscillating field giving rise to larger rf-induced steps; (c) the frequency of the external drive is more effective when it matches the ZFS resonance.

[1] R. Kleiner and P. Mueller, Phys. Rev. B **49**, 1327 (1994).
[2] R. Kleiner and P. Mueller, Phys. Rev. B **50**, 3942 (1994).
[3] A. Petraglia, A. Ustinov, N. F. Pedersen, and S. Sakai, J. Appl. Phys. **77**, 1171 (1995).
[4] A. V. Ustinov and H. Kohlstedt, Phys. Rev. B **54**, 6111 (1996).
[5] A. Wallraff, E. Goldobin, and A. V. Ustinov, J. Appl. Phys. **80**, 6523 (1996).
[6] A. C. Scott and A. Petraglia, Phys. Lett. A **211**, 161 (1996).
[7] G. Carapella and G. Costabile, Appl. Phys. Lett. **72**, 377 (1998).
[8] G. Carapella, G. Costabile, S. Sakai, and N.F. Pedersen, Phys. Rev. B **58**, 6497 (1998).
[9] S. Sakai, P. Bodin, and N. F. Pedersen, J. Appl. Phys. **73**, 2411 (1993).
[10] M. Salerno, M. Samuelsen, G. Filatrella, S. Pagano, and R. D. Parmentier, Phys. Lett. A **137**, 75 (1990); Phys. Rev. B **41**, 6641 (1990).
[11] A. Davidson and N. F. Pedersen, Phys. Rev. B **41**, 178 (1990).
[12] M. R. Samuelsen and S. A. Vasenko, *LT-17 (Contributed papers)*, edited by U. Eckern *et al.* (Elsevier Science, Amsterdam, 1984), p. 469.
[13] G. Costabile (private communication).